Available online at www.sciencedirect.com
SCIENCE DIRECT®

ELSEVIER

Dyes and Pigments 61 (2004) 149–164

DYES and PIGMENTS
www.elsevier.com/locate/dyepig

Application of experimental design for optimization of physicochemical properties of the inorganic pigment, iron(III) silicate

Mariusz B. Bogacki*, Iwona Michalska, Andrzej Krysztafkiewicz

Institute of Chemical Technology and Engineering, Poznań University of Technology, Pl.Curie-Skłodowskiej 2, 60-965 Poznań, Poland

Received 23 November 2001; received in revised form 19 January 2003; accepted 4 February 2003

Abstract

Optimization of physicochemical properties (bulk density, D_n, capacity to absorb water, H_w, capacity to absorb paraffin oil, H_o) of highly dispersed precipitated iron(III) silicate was performed, as related to temperature (T), flow rate of sodium metasilicate solution (v) and concentration of metal salts (c). The analysis was performed in three consecutive stages: (1) testing of silicate properties as affected by individual variables of the process, (2) empirical optimization, (3) experimental corroboration of the optimization. At each of the stages, appropriate experimental design was set up, mathematical model was established to describe the studied properties of silicate and statistical analysis of results was performed. The studies permitted to define optimum variables of precipitation of highly dispersed iron(III) silicate from sodium metasilicate solution using salt solution. Increase in precipitation temperature was found to bring about a decrease in bulk density and increases in capacities to absorb water and oil by the formed iron(III) silicate. Increase in the flow rate of sodium metasilicate solution induced a decrease in capacities to absorb water and oil and an increase in iron(III) silicate bulk density. On the other hand, increased concentration of iron(III) sulphate solution resulted in increased bulk density and capacity to absorb water but a decreased capacity to absorb oil by iron(III) silicate. This showed that individual properties of the formed silicate are related in various, sometimes opposite, ways to conditions of silicate precipitation. In the study the potential was demonstrated of applying factorial and compound designs for optimization of processes. The experimental optimization involved in parallel three different physicochemical properties: bulk density, capacity to absorb water and capacity to absorb paraffin oil. The properly planned and conducted experiment was shown to determine optimum conditions for conducting the process in cases when models describing the tested properties exhibit no extremum while variables of conducting the process exert opposite effects on the studied properties.

Keywords: Iron(III) silicate; Optimization; Precipitation of silicate; Highly dispersed inorganic pigments

---

* Corresponding author.
E-mail address: mariusz.bogacki@put.poznan.pl (M.B. Bogacki).

0143-7208/03/$ - see front matter © 2003 Elsevier Ltd. All rights reserved.
doi:10.1016/S0143-7208(03)00029-9

1. Introduction

Apart from providing color and covering the base, coats also protect the base against damaging effects of water, atmospheric agents, air polluting substances, salts, microbes and other [1]. Coat properties reflect properties of the paint components such as pigments, fillers, binding agents, solvents and diluents and numerous modifying supplements.

Apart from binding agents, inorganic pigments form principal components of coating materials. They play several important roles: they provide color of the coat, appropriate coating ability and protective capacities increasing its resistance to ultraviolet radiation and humidity. Due to the type of substances, which constitute the components, two types of pigments can be distinguished:

- homogeneous pigments, containing the same type of pigment particles, e.g. colorful metal oxides, metallic powders, etc.;
- mixtures, obtained either by chemical coating by the stain of an appropriate carrier such as the active, highly dispersed silica [2], precipitated calcium carbonate or by mechanical mixing of intensely staining pigment with a filler.

In modern façade paints, formed on the basis of silicate binding agent, inorganic metal silicates are used as pigments [3,4]. As compared to organic pigments they are more chemically neutral, resistant to elevated temperatures and to extreme pH of the environment. Silicate pigments can be obtained by precipitation from sodium metasilicate solution.

Covering power of a coat and its potential of providing uniform color reflect homogeneous distribution of a pigment. The corresponding potential is determined by an appropriate size of particles [5,6]. Therefore, the as low as possible bulk density represents one of significant properties, which characterize silicate, pigments. Low bulk density denotes high specific area of a given material and, which is particularly significant, its lower porosity.

Silicate paint as a purely mineral composition exhibits capillary activity [7]. The trait denotes the potential for absorbing water by such coats, which is equivalent to deterioration of their protective properties [2]. Therefore, the applied silicate pigments should exhibit possibly lowest capacity to absorb water and, thus, highly hydrophobic character. As exemplified by this study, the latter can be measured by the potential to absorb paraffin oil.

The important metal silicate properties, including bulk density (D_n), capacity to absorb water (H_w) and capacity to absorb oil (H_o) reflect precipitation conditions, including:

1. temperature (T), which may vary between 20 and 95 °C,
2. flow rate of sodium metasilicate solution (p), which may vary between 1 and 15 cm^3/min,
3. concentration of metal salts (c) with the variation range of 1.5–10%.

Thus, optimum values should be found for three different functions (D_n, H_w and H_o), dependent upon three different variables (T, v and c). In the first two cases function minimum is sought while in the third case maximum value of the function is searched for. Such optimization, involving three optimized functions (D_n, H_w, H_o) dependent on the same variables (T, v and c), may create significant difficulties, particularly when change in one of the analyzed variables will improve some of the interesting us physicochemical properties while it will markedly deteriorate the other properties. This may result in equivocal solutions and may require optimization and choice of approximate solutions.

Another problem involves selection of an optimum temperature in the metal silicate precipitation process. The till now performed studies [8–12] on the topic point to the need of employing high temperatures in the process. For economic reasons, however, the potential for conducting silicate precipitation in lower temperatures should be sought. For this reason, two variants of empirical optimization were applied. In the first variant, all variables of the process, including temperature, were changed. In the other variant the temperature was set at $T = 50$ °C while the other variables (flow rate of sodium metasilicate solution and salt concentration) were changing in order to obtain silicates of properties resembling those of products obtained in the first variant.

The present study aimed at (1) working out a procedure for parallel optimization of several important physicochemical properties depending on the same variables, and (2) selection of such variables of conducting the iron(III) silicate precipitation process (temperature, iron(III) salt concentration, flow rate of sodium metasilicate solution) that the obtained silicate would show optimum physicochemical properties, i.e., the lowest bulk density, low capacity to absorb water and high capacity to absorb paraffin oil.

2. Theory

Individual variables (temperature *T*, flow rate *v* and salt concentration *c*), the effects of which on silicate properties were examined, vary in different ranges. In particular, the range of temperature variations is much more extensive than those for the remaining variables. In such a case, standardization of variables was applied to balance off effects of individual variables on optimized properties.

The standardized variables are nondimensional and their values change within the range of [−1, 1]. They are determined according to the following formula:

$$t_i = \frac{x_i - x_i^0}{\Delta x_i}, \quad i = 1, 2, 3 \qquad (1)$$

where t_i is a standardized variable, corresponding to the natural variable *T, v* or *c* for *i* equal 1, 2 or 3, respectively; x_i represents one of the natural variables *T*, *v* or *c*; x_i^0 represents position of the central point in the vicinity of which the experiment is conducted; Δx_i represents an absolute step value along the $0x_i$ axis in the natural scale.

Optimization of silicate physicochemical properties was conducted in three consecutive stages:

1. estimation of iron(III) silicate properties as affected by variables of the precipitation process, in order to determine direction of changes and size of the function gradients in individual directions (stage **I**),
2. execution of 4–5 optimization steps in a direction indicated by function gradients, determined in the preceding stage (stage **II**),
3. experimental corroboration of the optimization, aimed at verifying the established optimum point (stage **III**).

Experiments conducted in the first stage conformed to the orthogonal 2^n two-level factorial design, where $n = 3$, of the form presented in Table 1 [13–15]. The design permits us to determine independently individual parameters of the polynomial model (2). According to the design, 8 experiments should be performed in which individual variables t_1, t_2 and t_3 are given code values at the upper (+1) and lower (−1) levels. In Table 1, the additional t_0 column acquires values at the upper level. This variable corresponds to the free term (a_0) in the determined linear model and it has been added to Table 1 for formal reasons.

The obtained results permitted to denote, using the least square method [16], three distinct linear models (each for a distinct studied property of the silicate) of the following form:

$$y^s(\mathbf{a}^s; \mathbf{t}) = a_0^s + a_1^s t_1 + a_2^s t_2 + a_3^s t_3, \quad s = 1, 2, 3 \qquad (2)$$

where: y^s denotes the foreseen by the model value of the studied property D_n, H_w and H_o for *s* equal 1, 2 or 3, respectively; $\mathbf{a}^s = \{a_0^s,\ a_1^s,\ a_2^s,\ a_3^s\}$ are parameters of the model constructed for D_n, H_w and H_o; $\mathbf{t} = \{t_1,\ t_2,\ t_3\}$ is the vector of coded variables, corresponding, in sequence, to temperature, *T*, flow rate of sodium metasilicate solution, *v*, and salt concentration, *c*.

Parameters a_1^s, a_2^s and a_3^s represent in parallel gradients of y^s function in vicinity of the design central point, x_i^0 in directions t_1, t_2 and t_3, respectively. They demonstrate effects of conditions (variables) (*T*, *v* or *c*) of conducting the silicate precipitation process on the studied properties.

The so obtained gradient values were applied at the second stage of empirical optimization, which included 4–5 experiments (Table 2). At this stage of the studies, the central point of the previous plan, i.e. the point at which coded variables t_1, t_2 and t_3 acquired 0 value (experiment 9), provided the starting point. Consecutive experiments were conducted in directions determined by gradients of individual functions. The step, at which variable (DT, Dv and Dc) values were accepted for, respectively, temperature, flow rate of sodium metasilicate solution and salt concentration was proportional to values of gradients of individual functions. Consecutive experiments were performed as long as changes in physicochemical properties (of the product) took place in the direction of interest. After the optimum point was reached, the subsequent experiment, resulting in deterioration of the properties, terminated this stage of studies.

Selection of the step at which one can transplace within the studied space was of particular importance. The step should be sufficiently small to reach the optimum point in 3–4 steps, starting at the point of origin. Such a step can warrant that the number of experiments performed at the stage is not exceedingly high and, on the other hand, pinpointing of the optimum point is sufficiently precise.

Table 1
Two-level factorial design of experiment for three variables applied at the first stage of studies; + and − denote values of variables coded at the upper and lower level, respectively

Experiment No.	t_0	t_1	t_2	t_3
1	+	+	+	+
2	+	−	+	+
3	+	+	−	+
4	+	−	−	+
5	+	+	+	−
6	+	−	+	−
7	+	+	−	−
8	+	−	−	−

Table 2
Design of experiment used in empirical optimization (second stage of studies). DT, Dv and Dc are working steps at which temperature T, flow rate of sodium metasilicate solution v and concentration of metal salt solution c, respectively, are modified

Experiment No.	t_1	t_2	t_3
9	0	0	0
10	DT	Dv	Dc
11	2DT	2Dv	2Dc
12	3DT	3Dv	3Dc
13	4DT	4Dv	4Dc

Another problem associated with step selection reflected the fact that effects of variables of silicate precipitation process on silicate properties were not identical (Table 6). For example, increase in temperature resulted in a decrease in bulk density and in capacity to absorb oil or in favorable alterations of silicate physicochemical properties but, in parallel, it induced an increase in the capacity to absorb water, e.g. increase in the property which should be as small as possible. Similarly equivocal were effects of the remaining variables on silicate properties.

In such a situation, the step at which individual variables (conditions) of conducting the process are altered should be selected in such a way that unfavorable alterations in silicate properties induced by changes in one variable are compensated by results of altering the remaining variables. In such a way, balancing the effects of individual variables on the studied properties, the step at which the variables are altered should be so selected that favorable alterations of all three properties can be obtained.

In order to verify position of the optimum point, defined at the second stage of the studies consecutive polynomial quadratic models were worked out, using the least square method:

$$y^s(\mathbf{a}^s;\mathbf{t}) = a_0^s + a_1^s t_1 + a_2^s t_2 + a_3^s t_3 + a_{12}^s t_1 t_2 + a_{13}^s t_1 t_3 + a_{23}^s t_2 t_3 + a_{11}^s t_1^2 + a_{22}^s t_2^2 + a_{33}^s t_3^2 \tag{3}$$

where $s=1, 2, 3$ denotes parameters for the models describing bulk density D_n, capacity to absorb water H_w and capacity to absorb paraffin oil H_o, respectively.

In this aim at the third stage experiments were conducted in line with the central composite design [15]. The design was constructed on the basis of a 2^3 two level factorial design supplemented by $2n$ axial or star runs and repetitions in the central point (Table 3). According to the design, 20 experiments should be performed, including 8 experiments of the basic two-level factorial design (experiments 14–21), six experiments in the star points (experiments 22–27) and six so called repetitions in the central point (experiments 28–33). Star points were located on t_1, t_2 and t_3 axes, separated by the so called star radius r from the central point of the plan. Value of the radius and number of repetitions were so selected that an orthogonal-rotatable plan was obtained. This indicated that variance of values, estimated in the model determined by the so accepted design, acquires the same value at equal distances from the central point of the design.

The obtained models [Eq. (3)], describing physicochemical properties of the silicate, were used to identify appropriate minima and maxima. In this aim, derivatives of the function (3) in respect to studied variables were approximated to zero obtaining three systems of linear equations with three unknowns:

$$\begin{aligned} a_1^s + 2a_{11}^s t_1 + a_{12}^s t_2 + a_{13}^s t_3 &= 0 \\ a_2^s + a_{12}^s t_1 + 2a_{22}^s t_2 + a_{23}^s t_3 &= 0 \\ a_3^s + a_{13}^s t_1 + a_{23}^s t_2 + 2a_{33}^s t_3 &= 0 \end{aligned} \tag{4}$$

Table 3
Central composite design of experiment used at the IIIrd stage of studies (star radius, $r = 1.682$, number of repetitions $N_0 = 6$, selected to obtain an orthogonal rotatable design)

Experiment No.	t_0	t_1	t_2	t_3
14	+	+	+	+
15	+	−	+	+
16	+	+	−	+
17	+	−	−	+
18	+	+	+	−
19	+	−	+	−
20	+	+	−	−
21	+	−	−	−
22	+	r	0	0
23	+	−r	0	0
24	+	0	r	0
25	+	0	−r	0
26	+	0	0	r
27	+	0	0	−r
28	+	0	0	0
29	+	0	0	0
30	+	0	0	0
31	+	0	0	0
32	+	0	0	0
33	+	0	0	0

where $s = 1, 2, 3$ denotes parameters for the models describing bulk density D_n, capacity to absorb water H_w and capacity to absorb paraffin oil H_o, respectively.

Solutions of the above equation system determine position of the stationary point of function (3). Attempting to find out if the points in fact represent extremum of the function and, if so, attempting to find out whether it involves a minimum or maximum one should check whether quadratic forms linked with the models are positively or negatively definite. The indispensable and sufficient condition for the quadratic form being positively definite was formulated by Sylvester [17]. According to the author, a quadratic form is positively definite when a sequence of inequalities (5) is fulfilled:

$$a_{11}^s > 0, \quad w_2 = \begin{vmatrix} a_{11}^s & \frac{1}{2}a_{12}^s \\ \frac{1}{2}a_{12}^s & a_{22}^s \end{vmatrix} > 0,$$

$$w_3 = \begin{vmatrix} a_{11}^s & \frac{1}{2}a_{12}^s & \frac{1}{2}a_{13}^s \\ \frac{1}{2}a_{12}^s & a_{22}^s & \frac{1}{2}a_{23}^s \\ \frac{1}{2}a_{13}^s & \frac{1}{2}a_{23}^s & a_{33}^s \end{vmatrix} > 0 \tag{5}$$

On the other hand, a quadratic form is negatively definite when the sequence of inequalities (6) is fulfilled, in which the > sign is substituted by the < sign in the first and the third inequality, i.e. when:

$$a_{11}^s < 0, \quad w_2 = \begin{vmatrix} a_{11}^s & \frac{1}{2}a_{12}^s \\ \frac{1}{2}a_{12}^s & a_{22}^s \end{vmatrix} > 0,$$

$$w_3 = \begin{vmatrix} a_{11}^s & \frac{1}{2}a_{12}^s & \frac{1}{2}a_{13}^s \\ \frac{1}{2}a_{12}^s & a_{22}^s & \frac{1}{2}a_{23}^s \\ \frac{1}{2}a_{13}^s & \frac{1}{2}a_{23}^s & a_{33}^s \end{vmatrix} < 0 \tag{6}$$

In such a situation the function attains its maximum in the studied stationary point. In cases when the quadratic form in question remains neither positively nor negatively defined, i.e. when neither of the inequality sequences (5) and (6) is fulfilled, Eq. (3) exhibits no extrema. In such a case the highest and the lowest values of the function (3) are positioned at the edges (extremes) of the studied region.

In cases when effects of variables, at which the precipitation process is conducted, on properties of the obtained metal silicate are equivocal, i.e., when changes in the variables result in favorable alterations of some properties and in unfavorable alterations of other properties of the product, a compromise solution has to be found. This indicates that such conditions of performing the silicate precipitation process should be found at which product of possibly best properties is obtained. In order to find such a solution, the following objective function has been suggested:

$$F(t_2, t_3; t_1) = \frac{y^1(\mathbf{a}^1; \mathbf{t}) - \min\limits_{t_1 \in [-1.5, 1.5]} y^1(\mathbf{a}^1; \mathbf{t})}{\max\limits_{t_1 \in [-1.5, 1.5]} y^1(\mathbf{a}^1; \mathbf{t}) - \min\limits_{t_1 \in [-1.5, 1.5]} y^1(\mathbf{a}^1; \mathbf{t})} w_1 + \frac{y^2(\mathbf{a}^2; \mathbf{t}) - \min\limits_{t_1 \in [-1.5, 1.5]} y^2(\mathbf{a}^2; \mathbf{t})}{\max\limits_{t_1 \in [-1.5, 1.5]} y^2(\mathbf{a}^2; \mathbf{t}) - \min\limits_{t_1 \in [-1.5, 1.5]} y^2(\mathbf{a}^2; \mathbf{t})} w_2 + \frac{\max\limits_{t_1 \in [-1.5, 1.5]} y^3(\mathbf{a}^3; \mathbf{t}) - y^3(\mathbf{a}^3; \mathbf{t})}{\max\limits_{t_1 \in [-1.5, 1.5]} y^3(\mathbf{a}^3; \mathbf{t}) - \min\limits_{t_1 \in [-1.5, 1.5]} y^3(\mathbf{a}^3; \mathbf{t})} w_3, \quad (7)$$

In the function, t_2 and t_3 variables are treated as parameters acquiring the values of ±1 while $t_1 \in [1.5, 1.5]$ represents a independent variable, weights $w_i \in [0, 1]$, $i = 1, 2, 3$ serve to indicate traits which are particularly significant for the investigator. Individual terms of the function (7) are related, respectively, to bulk density D_n, capacity to absorb water H_w, capacity to absorb paraffin oil H_o. Each of the terms is given values from the [0, 1] interval, 0 corresponding to conditions in which given property exhibits most desired value while 1 corresponding to unfavorable value of the property. In effect, the entire function carries values from the $[0, \Sigma w_i]$ interval. Minimum of the function corresponds to such conditions of conducting the process in which the precipitated metal silicate exhibits optimum properties (in respect to the objective function 7).

3. Experimental

Precipitation of highly dispersed iron(III) silicate was performed in a spherical flask of 500 cm^3 capacity. In the flask, salt solution (iron(III) sulphate, POCh, Gliwice, Poland) of the required concentration c was placed. In a stand, a rapidly revolving mixer was fixed and the flask was placed in a thermostat to continuously control the temperature T. The precipitating agent, sodium metasilicate solution (Vitrosilicon S.A., Iłowa, Poland), contained 27.18% SiO_2, 8.5% Na_2O and manifested density of 1.39 g/cm^3, module 3.3. It was fed using a peristaltic pump at a stable flow rate, v. The precipitating agent was added up to the moment of complete silicate precipitation from the reaction solution. In the course of adding sodium metasilicate, pH of the solution increased from around 2 (for pure salt) to 10. In the studies attainment of such a pH level signalised the end of the precipitation process. The obtained sediment of metal silicate was separated from the post-reactive mix by Büchner funnel filtration under suction and, then, washed with water to rinse off the remains of the salt. The sample was dried in a stationary drier at 105 °C for 2 h. While drying, the sediment was fluffed several times to prevent agglomerate formation. The dried silicate was ground in an electric mortar (type 02, Frisch Pulverisette, Germany) to provide it with appropriate looseness and fineness of grinding and it was passed through a 0.063 mm sieve. The so obtained silicates were subjected to physicochemical tests.

Bulk density was determined in a graduated cylinder of a known capacity. Using a funnel, the cylinder was filled with the pre-sieved silicate until a cone was formed on its top. The cone was flattened to the upper edge of the cylinder and the cylinder was weighed. Bulk density was determined as a difference in weight of the filled and the empty cylinder.

Capacities to absorb water and oil were estimated by addition of distilled water or of paraffin oil from a microburette to 0.2 g silicate sample, which was earlier passed through a sieve and placed on a ceramic plate. Upon addition of consecutive drops of the fluid, the sample was ground using a steel spatula to obtain a homogeneous paste. The end point of determination of absorbing capacities was noted when an excess of a single drop of distilled water or paraffin oil abruptly changed consistency of the paste, resulting in its evident fluidization.

Determinations of bulk densities, capacities to absorb water and oil were repeated thrice for each sample of metal silicate and a mean value was calculated. This permitted to calculate relative errors of the measurements (Table 5). The lowest error was associated with measuring of bulk density (1.6 to 3.2%). Determinations of water- and oil-absorbing capacities were associated with a larger error, which amounted to 5.2–10.2% and 5.2–10.5%, respectively.

4. Results and discussion

4.1. First and second stages of studies

Experiments conducted at the stage I aimed at determining gradients for individual functions, describing examined properties of the silicate. The experiments were performed as presented in the factorial schedule presented in Table 1. The values which characterized the schedule, in particular positions of points at the upper (+) level and the lower (−) level, are given in Table 4. The table presents also natural values of temperature T, flow rate of sodium metasilicate solution v and concentrations of metal salts c. The obtained experimental results are listed in Table 5. Regression coefficients for linear models [Eq. (2)], describing bulk density (D_n), capacities to absorb water (H_w) and paraffin oil (H_o), are given in Table 6. The table presents also correlation coefficient (R^2) values for individual models. Results of optimization experiments for iron(III) silicate (II stage of studies) are presented in Tables 7 and 8.

Analysis of coefficients of the linear model [Eq. (2)], describing the relation between bulk density on one hand and temperature, salt concentration and flow rate on the other (Table 6) demonstrates that increase in temperature and concentration of iron(III) silicate concentration (parameters a_1 and a_3) should result in a decreased bulk density (D_n) of iron(III) silicate. Positive value of a_2 parameter in the model demonstrates, in turn, that flow rate of metasilicate sodium should be decreased to obtain iron silicate of a lower bulk density. A similar effect of the three factors can be observed in the case of the capacity to absorb oil (H_o). In

Table 4
Values which characterize the applied experimental designs in studies on physicochemical properties of iron(III) silicate and applied at the Ist and IIIrd stages of studies

	Iron(III) silicate		
Symbol	T (°C)	v (cm^3/min)	c (%)
+	80	10.0	5.0
−	20	1.2	2.5
x^0	50	5.6	3.75
Δx	30	4.4	1.25
+	70	4.5	3.8
−	30	2.5	3.0
$+r$	83	5.2	4.1
$-r$	16	1.8	2.7
X^0	50	3.5	3.4
Δx	20	1.0	0.4

Table 5
Properties of iron(III) silicate obtained at the Ist stage of studies (number of experiments are consistent with data of Table 1; relative error $\frac{x_i-\bar{x}}{\bar{x}}$%: (a) the lowest relative error, (b) the highest relative error

Experiment No.	Iron(III) silicate		
	D_n (g/dm^3)	H_w (cm^3/100 g)	H_o (cm^3/100 g)
1	220	140	305
2	405	60	165
3	195	170	325
4	360	80	210
5	285	100	280
6	410	65	160
7	275	100	300
8	375	80	190
(a)	1.6	5.2	5.2
(b)	3.2	10.5	10.5

Table 6
Regression coefficients of linear models [Eq. (13)], describing physicochemical properties of iron(III) silicate (R^2—correlation coefficient)

Parameter	Iron(III) silicate		
	D_n (g/dm^3)	H_w (cm^3/100 g)	H_o (cm^3/100 g)
a_0	315.6	99.4	241.9
a_1	−71.9	28.1	60.6
a_2	14.4	−8.13	−14.4
a_3	−20.6	13.1	9.38
R^2	0.9762	0.9020	0.9955

order to obtain iron silicate of high capacity to absorb oil, the precipitation process should be conducted at an elevated temperature and at higher concentrations of iron(III) sulphate while the flow rate should be decreased. The exactly opposite effect can be observed in the case of the capacity of iron silicate to absorb water (H_w). In order to obtain product of a low water-absorbing capacity, the precipitation should be performed at a relatively low temperature and at a possibly lowest concentration of iron(III) sulphate. On the other hand, sodium metasilicate flow rate should be as high as possible. Thus, opposing effects of the analyzed factors have been observed on physicochemical properties of iron silicate.

Comparison of absolute values of the estimated function gradients (Table 6) demonstrates a particularly pronounced effects of temperature on properties of iron silicate, as compared to effects of flow rate and salt concentration. The effects are particularly high in cases of bulk density and capacity to absorb oil and definitely less pronounced although still significant in the case of water-absorbing capacity. For this reason, upon experimental optimization attempts (stage II) effects the coded value defined ($DT=0.2$) increase in temperature, which unfavorably affects water-absorbing capacity, have been assumed to be compensated by a decrease in concentration in iron(III) sulphate ($Dc=-0.4$) and an increase in sodium metasilicate flow rate ($Dv=0.1$). In accordance with the equation **2**, such changes in values of individual factors should result in favorable alterations in physicochemical properties of the product: $\Delta D_n=-4.69$; $\Delta H_w=-0.44$; $\Delta H_o=6.94$). Thus, such changes can be expected to result in a marked decrease in bulk density and a slight decrease in water-absorbing capacity with a parallel significant increase in oil-absorbing capacity.

In the second variety of optimization, the temperature has been assumed to remain constant (50 °C, $DT=0$), accompanied by decreased flow rate and salt concentration ($Dv=-0.15$; $Dc=-0.1$). In accordance with Eq. (2), such alterations should induce the following changes in physicochemical properties of the product: $\Delta D_n=-0.09$; $\Delta H_w=-0.09$; $\Delta H_o=1.2$).

Thus, particularly extensive changes can be expected in the case of oil-absorbing capacity, while alterations in capacity to absorb water and in bulk density should be comparable and relatively small. Nevertheless, also in this case the observed alterations in physicochemical properties should take place in the favorable direction: bulk density and capacity to absorb water should decrease, paralleled by increasing oil-absorbing capacity.

Table 7
Variables of the IInd stage of studies and physicochemical properties of iron(III) silicate (the variant with variable temperature)

Experiment No.	Variables			Properties		
	T (°C)	v (cm^3/min)	c (%)	D_n (g/dm^3)	H_w (cm^3/100 g)	H_o (cm^3/100 g)
9	40	5.6	3.7	325	100	275
10	45	6.0	3.2	292	125	275
11	50	6.4	2.7	250	100	300
12	55	6.8	2.2	250	100	300
13	60	7.2	1.7	265	150	300

Table 8
Variables of the IInd stage of studies and physicochemical properties of iron(III) silicate (the variant with temperature set at 50 °C)

Experiment No.	Variables			Properties		
	T (°C)	v (cm^3/min)	c (%)	D_n (g/dm^3)	H_w (cm^3/100 g)	H_o (cm^3/100 g)
9′	50	5.6	3.7	240	150	300
10′	50	4.9	3.6	223	225	300
11′	50	4.2	3.5	177	175	350
12′	50	3.5	3.4	163	150	375
13′	50	2.8	3.3	165	175	375

Analysis of the results of stage II of the optimization (Table 7) indicates that desirable alterations in physicochemical properties of iron silicate have taken place in three consecutive experiments (experiments 9–11). After the optimum parameters have been reached (experiments 11 and 12), iron silicate obtained in the consecutive experiment (experiment 13) has already demonstrated less advantageous properties. Also the iron silicates obtained in the four consecutive experiments with stable temperature (Table 8) have manifested increasingly favorable properties. The silicates also have shown lower bulk density and higher capacity to absorb oil as compared to silicates obtained in the variety with a variable temperature. On the other hand, they show an increased potential to absorb water. Since oil-absorbing capacity and bulk density represent particularly significant properties of the product, the point 12′ has been accepted to serve as a central point of the composition schedule (stage III).

Table 9
Properties of iron(III) silicate obtained at the IIIrd stage of optimisation (numbers of experiments consistent with those in Table 3)

Experiment No.	Iron(III) silicate		
	D_n (g/dm^3)	H_w (cm^3/100 g)	H_o (cm^3/100 g)
14	179	200	425
15	344	125	225
16	200	150	325
17	322	125	250
18	244	150	350
19	370	100	225
20	181	160	400
21	249	100	300
22	222	200	325
23	385	100	200
24	228	175	350
25	206	125	250
26	263	150	250
27	245	200	350
28	217	175	375
29	204	150	375
30	177	150	375
31	210	150	350
32	200	175	375
33	210	150	350

Table 10
Regression coefficients of quadratic models [Eq. (3)], describing physicochemical properties of iron(III) silicate (R^2—correlation coefficient)

Parameter	Iron(III) silicate		
	D_n (g/dm^3)	H_w (cm^3/100 g)	H_o (cm^3/100 g)
a_0	203.1	158.7	366.1
a_1	−54.7	27.5	51.4
a_2	16.2	9.0	−3.7
a_3	2.8	−6.9	−27.4
a_{12}	−12.6	5.0	18.8
a_{13}	−11.6	−13.8	−12.5
a_{23}	−22.9	−5.0	6.3
a_{11}	35.3	−7.0	−33.9
a_{22}	5.1	−7.0	−3.5
a_{33}	17.4	1.9	−20.7
R^2	0.9824	0.9108	0.9723
a_{11}	35.3	−7.0	−33.9
w_2	139.8	42.2	29.4
w_3	−3194	541.2	−509.3
*	–	–	Max

4.2. Stage III

Stage III of the studies has involved verification of the earlier established optimum points. The studies have been performed in accordance with the composition schedule (Table 3). Values which characterize the schedule, including position of the central point of the schedule (x^0) and size of star radius (r) are given in Table 4. The optimum point, established at stage II, has been accepted to represent central point of the schedule. Results of the performed experiments are given in Table 9. Using the obtained results, polynomial models have been constructed [Eq. (3)], describing bulk density (D_n), capacity to absorb water (H_w), and capacity to absorb paraffin oil (H_o). Values of regression coefficients for individual models, coefficients of determination (R^2) and values of determinants used to find out whether the constructed models are positively or negatively definite (inequalities 5 and/or 6) are given in Table 10.

The models, which describe physicochemical properties of iron(III) silicate as function of conditions in which precipitation is conducted fit well the experimental data. This has been demonstrated both by values of correlation coefficients (R^2), given in Table 10, and by comparison of silicate properties calculated from appropriate models with experimental data (Fig. 1a–c).

The constructed models (Table 10), describing bulk density (D_n), water-absorbing capacity (H_w) and oil-absorbing capacity (H_o) as related to conditions of iron(III) silicate precipitation, have been consistent with the experimental data. This has been demonstrated both by values of correlation coefficients (R^2) and by comparison of silicate

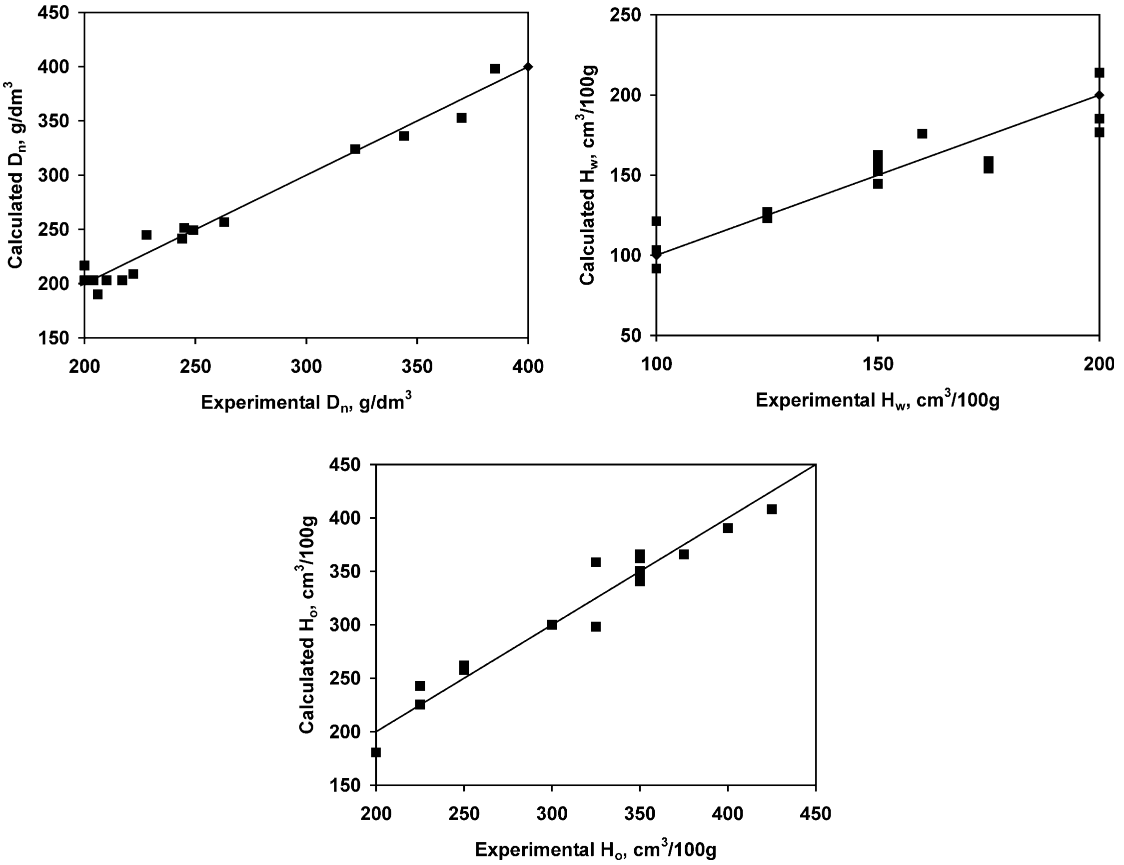

Fig. 1. Comparison of experimentally established physicochemical properties of iron(III) silicate with properties foreseen by model (3): (a) bulk density D_n; (b) capacity to absorb water H_w; (c) capacity to absorb paraffin oil H_o.

properties calculated by appropriate models with properties documented by respective experiments.

Determinant values for individual models (Table 10), calculated using Eq. (5) or (6), have permitted to find out that the models describing bulk density and capacity to absorb water are neither positively nor negatively definite. On the other hand, the model describing oil-absorbing capacity is negatively definite. This indicates that the former two models exhibit no extremum values but only the lowest and the highest values at the limits of the examined range of alterations. The third model manifests maximum value.

The situation is well characterized by cross-sections performed for individual models. In the case of bulk density, the cross-section shape resembles elongated gutter with a slight decline (Fig. 2). In

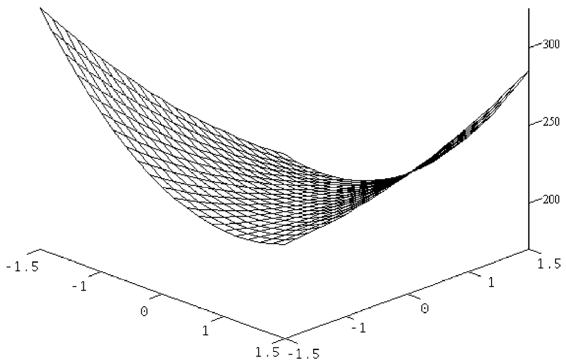

Fig. 2. Cross-section through the surface describing bulk density of iron(III) silicate representing a function of coded values of precipitation temperature $t_1 \in [-1.5; 1.5]$, flow rate of sodium metasilicate solution $t_2 \in [-1.5; 1.5]$ and of iron(III) sulphate concentration $t_3 \in [-1.5; 1.5]$. The cross-section is shown for the coded temperature value, $t_1 = 0$ ($T = 50$ °C).

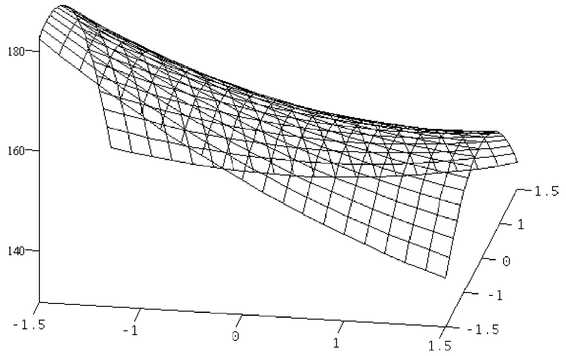

Fig. 3. Cross-section through the surface describing iron(III) silicate capacity to absorb water as a function of coded values of precipitation temperature $t_1 \in [-1.5; 1.5]$, flow rate of sodium metasilicate solution $t_2 \in [-1.5; 1.5]$ and of iron(III) sulphate concentration $t_3 \in [-1.5; 1.5]$. The cross-section is shown for the coded temperature value, $t_1 = 0$ ($T = 50$ °C).

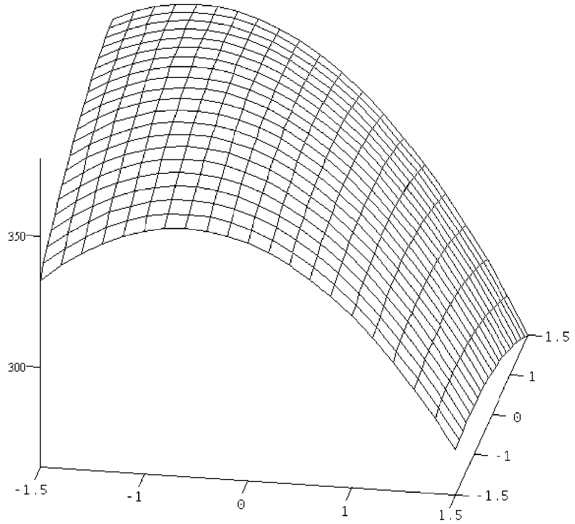

Fig. 4. Cross-section through the surface describing iron(III) silicate capacity to absorb oil as a function of coded values of precipitation temperature $t_1 \in [-1.5; 1.5]$, flow rate of sodium metasilicate solution $t_2 \in [-1.5; 1.5]$ and of iron(III) sulphate concentration $t_3 \in [-1.5; 1.5]$. The cross-section is shown for the coded flow rate of sodium metasilicate solution $t_2 = 0$ ($p = 3.5$ cm^3/min).

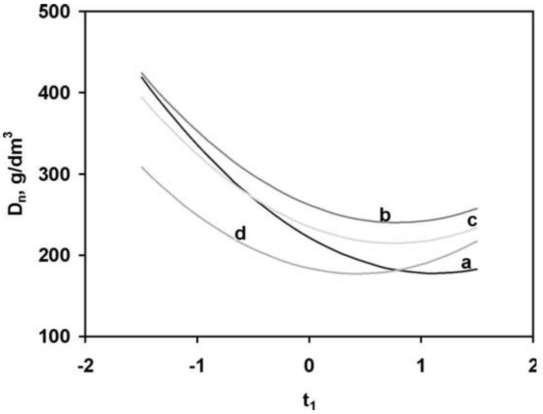

Fig. 5. Effect of temperature (t_1) on bulk density of iron(III) silicate The curves correspond to cross-sections at edges of the studied region of alterations: a: $t_2 = 1$, $t_3 = 1$; b: $t_2 = 1$, $t_3 = -1$; c: $t_2 = -1$, $t_3 = 1$; d: $t_2 = -1$, $t_3 = -1$.

the case of water-absorbing capacity the cross-section manifest the typical saddle shape (Fig. 3) while in the case of oil-absorbing capacity a marked maximum is observed (Fig. 4).

In order to determine maximum of oil-absorbing capacity the set Eq. (4) has been solved. Extremum of the model has been noted in the point of the following coded coordinates: $t_1 = 2.292$, $t_2 = 5.157$, $t_3 = -0.575$, which corresponds to the following natural values: temperature $T = 95.8$ °C, rate flow of sodium metasilicate solution $v = 8.7$ cm^3/min, iron(III) sulphate concentration $c = 3.2\%$. At this point, the model-estimated value oil-absorbing capacity has amounted to $H_o = 423$ cm^3/100 g and has resembled the best experimental results (Table 10).

Taking advantage of the remaining models, predicted values of bulk density ($D_n = 420$ g/dm^3) and of water-absorbing capacity ($H_w = 143$ cm^3/100 g) have been calculated in the point of the maximum oil-absorbing capacity. While the model-predicted water-absorbing capacity has been relatively low, fitting the experimentally established range, the model-predicted bulk density has proven very high (beyond the experimental range) and could not have been accepted. In such a situation, the point corresponding to maximum oil-absorbing capacity could not have been used as the optimum point.

Since the models which describe bulk density and capacity to absorb water exhibit no extrema, behavior of the functions should be examined at limits of the studied range. As shown in Figs. 5–7, independently of the accepted values of sodium metasilicate flow rate (t_2) and iron(III) sulphate concentration (t_3), the studied physicochemical properties behave in a similar manner: increase in temperature brings about a decrease in bulk density, which reach the lowest values for coded temperature values of the [0.0–1.0] range, while capacities to absorb water and oil increase.

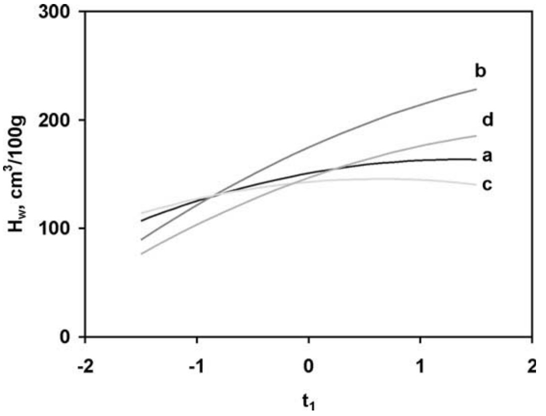

Fig. 6. Effect of temperature (t_1) on iron(III) silicate capacity to absorb water. The curves correspond to cross-sections at edges of the studied region of alterations: a: $t_2 = 1$, $t_3 = 1$; b: $t_2 = 1$, $t_3 = -1$; c: $t_2 = -1$, $t_3 = 1$; d: $t_2 = -1$, $t_3 = -1$.

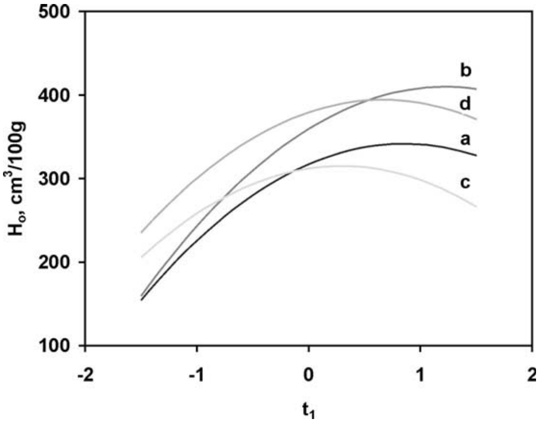

Fig. 7. Effect of temperature (t_1) on iron(III) silicate capacity to absorb oil; The curves correspond to cross-sections at edges of the studied region of alterations: a: $t_2 = 1$, $t_3 = 1$; b: $t_2 = 1$, $t_3 = -1$; c: $t_2 = -1$, $t_3 = 1$; d: $t_2 = -1$, $t_3 = -1$.

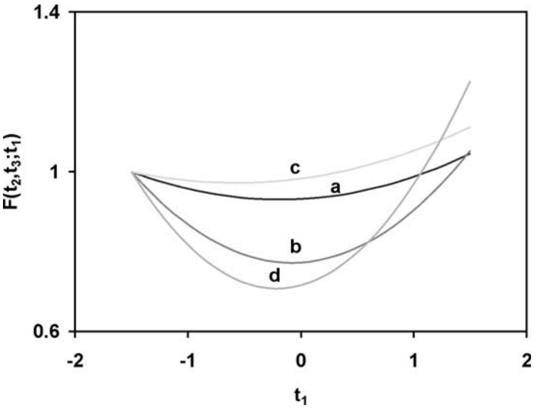

Fig. 8. Profile of objective function (7) as related to temperature (t_1) for various variables: a: $t_2 = 1$, $t_3 = 1$; b: $t_2 = 1$, $t_3 = -1$; c: $t_2 = -1$, $t_3 = 1$; d: $t_2 = -1$, $t_3 = -1$; $w = \{0.5, 1, 0.5\}$.

Table 11
Predicted physicochemical properties of iron(III) silicate for temperature $t_1 = 0$ ($T = 50$ °C) and four different values of flow rate (v) and iron(III) sulphate (c)

Process parameters						Properties of iron(III) silicate		
Temperature		Flow rate		Concentration of iron(III) sulphate				
t_1	T (°C)	t_2	v (cm^3/min)	t_3	c (%)	D_n (g/dm^3)	H_w (cm^3/100 g)	H_o (cm^3/100 g)
0	50	1	4.5	1	3.8	222	151	317
0	50	1	4.5	−1	3.0	262	175	359
0	50	−1	2.5	1	3.8	235	143	312
0	50	−1	2.5	−1	3.0	184	147	379

The increase in water-absorbing capacity taking place with increasing temperature has been practically monotonous while the capacity to absorb oil has declined after it reached maximum. Such a relation of properties of studied iron(III) silicate and of conditions of conducting the precipitation process indicates that while it is possible to define such conditions of precipitating iron(III) silicate that the product shows low bulk density and low oil-absorbing capacity, the parallel reduction of water-absorbing capacity may present serious difficulties.

Bulk density and capacity to absorb paraffin oil are similarly related to conditions of iron(III) silicate precipitation (Figs. 5–7). This indicates that the same precipitation conditions permit to obtain silicate of both low bulk density and low capacity to absorb oil. In this situation individual elements of the objective function (7) will sum up, resulting in excessive emphasis on production of silicate manifesting such properties and in neglecting effects of the conditions on water-absorbing capacity. In order to balance off the drawback, the weight set of $w = \{0.5; 1.0; 0.5\}$ has been applied to accentuate importance of water-absorbing capacity. Course of the respective objective function (7) in presented in Fig. 8.

Depending upon the accepted combination of coded values of sodium metasilicate solution flow rate and iron(III) sulphate concentration, the suggested function reaches its minimum for coded values of temperature t_1 within the range of [−0.15 to −0.10]. This indicates that the optimum

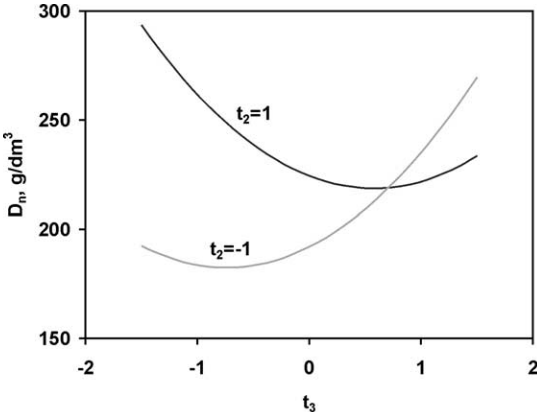

Fig. 9. Dependence of iron(III) silicate bulk density on salt concentration. The curves correspond to cross-sections at edges of the studied region of alterations; $t_1 = 0$; $t_2 = \{-1, 1\}$.

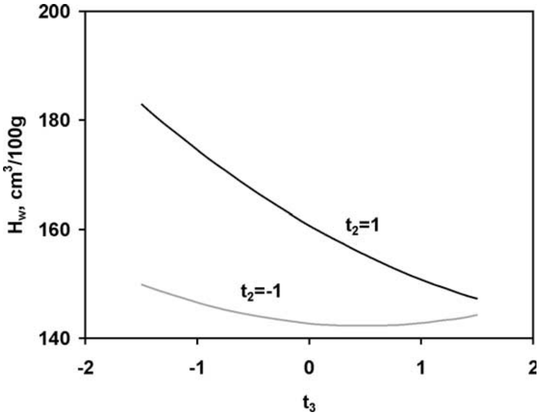

Fig. 10. Dependence of iron(III) silicate capacity to absorb water on salt concentration. The curves correspond to cross-sections at edges of the studied region of alterations; $t_1 = 0$; $t_2 = \{-1, 1\}$.

temperature for precipitation of iron(III) silicate should amount to 47–48 °C. In this situation, taking into account conditions of performing the experiment, the temperature of coded value $t_1 = 0$ has been accepted for further studies, corresponding to the natural value of $T = 50$ °C.

Physicochemical properties of iron(III) silicate, predicted for the accepted temperature and four varieties of the remaining precipitation parameters are presented in Table 11. Effects of sodium metasilicate solution flow rate and of iron(III) sulphate concentration on bulk density and capacity to absorb water can be noted exceed those on oil-absorbing capacity. The oil-absorbing capacity predicted for the suggested temperature ($T = 50$ °C) of precipitating iron(III) silicate has proven lower by 10-20% than the maximum value. Capacity to absorb water has shown low values and has not differed from the experimental values.

Bulk density, capacity to absorb water and capacity to absorb paraffin oil, as influenced by concentration of iron(III) sulphate concentration are presented in Figs. 9–11, calculated from respective models for the accepted temperature of $t_1 = 0$ and for sodium metasilicate flow rate of $t_2 = \{-1, 1\}$. Individual curves unequivocally demonstrate that iron(III) silicate of most favorable properties can be obtained employing sodium metasilicate solution flow rate at the lower level, i.e., accepting $t_2 = -1$.

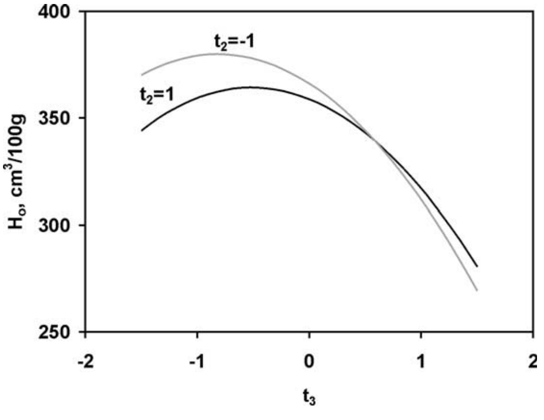

Fig. 11. Dependence of iron(III) silicate capacity to absorb oil on salt concentration. The curves correspond to cross-sections at edges of the studied region of alterations; $t_1 = 0$; $t_2 = \{-1, 1\}$.

However, definition of appropriate concentration of iron(III) sulphate concentration has proven to pose the greatest difficulty since the lowest value of bulk density and the highest capacity to absorb paraffin oil could have been obtained accepting t_3 within the range of [−0.5; 0.0] while the lowest capacity to absorb water could have been reached for $t_3 \in [0.0; 0.5]$ or on the opposite side of the central point.

Attempting to define levels of iron(III) sulphate concentration, employed for silicate precipitation, the objective function has been constructed, accepting values within the range of [0, Σw_i]. Salt concentration t_3 represents a dependent variable

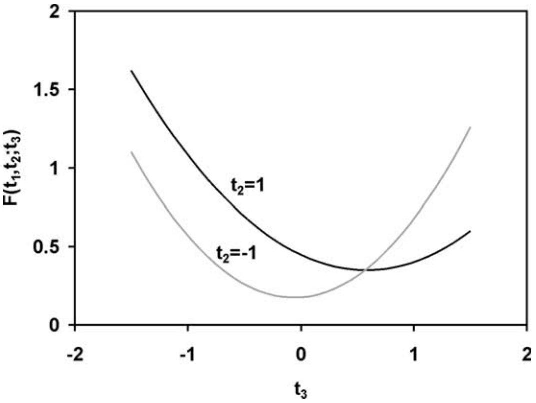

Fig. 12. Profile of objective function (7) as related to iron(III) concentration for various flow rates of sodium metasilicate solution; $t_1 = 0$, $t_2 = \{-1, 1\}$, $w = \{0.5, 1.0, 0.5\}$.

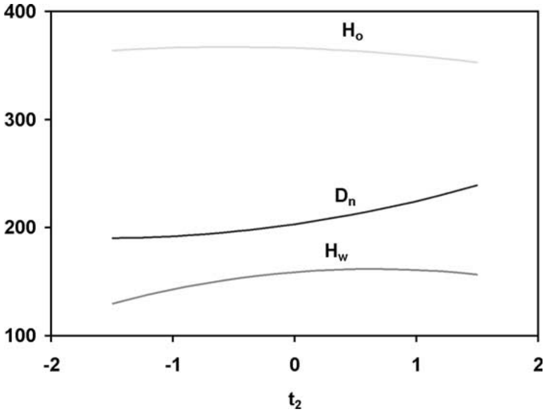

Fig. 13. Dependence of iron(III) silicate properties on flow rate of sodium metasilicate solution; $t_1 = 0$, $t_3 = 0$.

of the function while temperature $t_1 = 0$ and flow rate of sodium metasilicate solution $t_2 = \{-1, 1\}$ represent its parameters. Course of the function is shown in Fig. 12.

The function manifests the lowest values at $t_1 = 0$, $t_2 = -1$, $t_3 = 0.0$. This corresponds to real values of temperature $T = 50$ °C, flow rate of sodium metasilicate solution $v = 2.5$ cm^3/min and iron(III) sulphate concentration $c = 3.4\%$. At this point, the following properties of precipitated iron(III) silicate are predicted: $D_n = 192$ g/dm^3, $H_w = 143$ cm^3/100 g, $H_o = 366$ cm^3/100 g.

Changes in bulk density, capacity to absorb water and capacity to absorb paraffin oil, as dependent upon flow rate of sodium metasilicate solution t_2 for the temperature $t_1 = 0$ and salt concentration $t_3 = 0$ are shown in Fig. 13. Course of individual curves unequivocally corroborates results of the above performed analysis of effects exerted by individual parameters of iron(III) silicate precipitation on its properties and correctness of the conditions accepted for conducting the process in further studies.

In order to corroborate the conclusions, a verifying three experiments has been performed ($T = 50$ °C; $v = 2.5$ cm^3/min; $c = 3.4\%$) obtaining iron(III) silicate of the following properties: $D_n = 227$ g/dm^3, $H_w = 125$ cm^3 /100 g and $H_o = 320$ cm^3/100 g. The properties of the obtained iron(III) silicate have differed from those predicted by the model by around 10%–15%. This errors are nearly with the relative errors of the experimental determination (5–10%) This provides an evidence for the correctness of the applied mathematical models and of the optimization technique.

5. Conclusions

Increase in precipitation temperature induced a decrease in bulk density but increase in capacities to absorb water and oil by iron(III) silicate. Increase in flow rate of sodium metasilicate solution resulted in decreased capacities to absorb water and oil and in increased bulk density of iron(III) silicate. Increase in iron(III) sulphate concentration induced a decrease in bulk density but increases in capacities to absorb water and paraffin oil by the obtained iron(III) silicate. This indicated that various properties of metal silicate are related to conditions of their precipitation in various, sometimes opposite, manner.

In the study we demonstrated potential for employing factorial and composition schedules for optimization of the process. Experimental optimization was conducted in parallel for three distinct physicochemical properties, including bulk density, capacity to absorb water and capacity to absorb paraffin oil. An appropriately designed and executed experiment was demonstrated to define optimum conditions for conducting the process in cases when models describing the studied properties exhibit no extremum and effects of variables of conducting the process are opposite.

Acknowledgements

The study was partially subsidized by the promotor's grant from Polish Research Committee KBN, No.3T09BO5317, and partially by the grant DS 32/014/2001 from Poznań University of Technology.

References

[1] Karaszkiewicz P. Farba farbie nierówna. Renowacje 1998;3:8–16.

[2] Binkowski S, Jesionowski T, Krysztafkiewicz A. Preparation of pigments on modified precipitated silicas. Dyes and Pigments 2000;74:247–57.

[3] Garda C, Kacprzak F. Barwienia Tworzyw Sztucznych. Warszawa: WNT; 1966.

[4] Werner J. Podstawy Technologii Malarstwa i Grafiki. Warszawa: PWN; 1985. p. 14–35.

[5] Brown RFG, Carr C, Taylor ME. Effect of pigment volume concentration and latex particle size on pigment distribution. Progress in Organic Coatings 1997;30:185–94.

[6] Kobayashi T. Pigment dispersion in water-reducible paint. Progress in Organic Coatings 1996;28:79–87.

[7] Erfurth U. Farby na bazie żywic silikonowych—mity i rzeczywistość. Renowacje 1998;3:17–27.

[8] Jesionowski T, Krysztafkiewicz A. Production of highly dispersed sodium–aluminium silicate to be used as a white pigment or as a polymer filler. Pigments and Resin Technology 1996;25:4–14.

[9] Krysztafkiewicz A. Modified calcium silicates as active rubber fillers. Journal of Materials Science 1987;22:478–82.

[10] Krysztafkiewicz A. Modified zinc silicate—an active rubber filler. Journal of Materials Science 1988;23:2407–14.

[11] Bergna HE. The colloid chemistry of silica. In: Advances in chemistry series 234. American Chemical Society, 1994. p. 1–47.

[12] Anon. Katz HS, editor. Handbook of fillers and reinforcements for palastics. Van Nostrand Reinhold Company, 1987. p. 65–127.

[13] Box GEP, Hunter WG. The experimental study of physical mechanisms. Technometrics 1965;7(1):23–42.

[14] Atkinson AC, Donev AN. Optimum experimental designs. Oxford: Clarendon Press; 1992.

[15] Montgomery DC. Design and analysis of experiments. Wiley; 1997.

[16] Draper NR, Smith H. Applied regression analysis. 2nd ed. New York: Wiley; 1981.

[17] Fichtenholz GM. Rachunek różniczkowy i calkowy. Warszawa: Pań有stwowe Wydawnictwa Naukowe; 1976. p. 372–5.